Study of RF/DC co-sputtered TiAlN plasma using Langmuir probe for prospective Industrial applications

Ashwini Kumar Singh*, Neelam Kumari and P. K. Barhai

Department of Applied Physics, Birla Institute of Technology, Mesra, Ranchi-835215, INDIA

Abstract

Titanium Aluminium nitride thin films prepare by magnetron RF/DC co-sputtering system is commercially used for production of hard coatings for the industrial uses. Plasma parameter like plasma potential, floating potential, electron temperature, electron density and ion density plays vital role in defining the properties of the thin films. To understand these physical phenomenons, we have studied the plasma behavior with the help of Langmuir probe constructed by tungsten wire of small diameter. Several studies shows different type of relationship between these parameters with the plasma, but till date no study shows how these phenomenon are in particular responsible for the better properties and at what conditions best result should be obtained for industrial applications.

Keywords: Titanium aluminium nitride, Magnetron sputtering, Plasma Diagnostics, Langmuir Probe

IJERT

Nomenclature

A = Langmuir probe area, m^2

n_e = electron number density, m^{-3}

e = electron charge, C

k = Boltzmann constant

T_e = electron temperature, eV

T_i = ion temperature, eV

I_e = electron current, A

V_p = plasma potential, V

I_{es} = electron saturation current, A

V_e = electron Velocity, ms^{-1}

I_{is} = ion saturation current, A

V_i= ion Velocity, ms^{-1}

n_i = ion number density, m^{-3}

V_B= Probe voltage (V)

$f_e(\epsilon)$ = Electron energy distribution function (EEDF)

V_f = floating potential, V

1. Introduction

Reactive magnetron co-sputtering is widely used technique for the metal oxide and metal nitride surface coatings. In these types of devices magnetic and electrical fields are used in combination to achieve the specific properties due to the surface treatment/coating. Plasma species in the discharge are governed by the reaction of gases and metals in particular ratio due to the crossed magnetic and electrical fields, cathode (material used for sputtering), pressure, discharge power density and sputter gas used [1]. The nature of such plasma discharge is complex in nature and can be understood by monitoring the plasma parameters like density, temperature, energy etc. [2-4]. Magnetron sputtering process of thin film growth

is widely used for the applications like antireflection coatings, decorative/protective coatings, metallic interconnects in microelectronics, magnetic recording heads, thin film solar cells, etc. This plasma assisted process enhances the efficiency of deposition rate and is devoid of any chemical reactants so it is eco-friendly [5-8].

TiAlN thin films had found its use in the field of hard coating in last decades due to its high hardness (30-35GPa), oxidation resistance in the range (850-900^{0}C) and higher corrosion resistance. TiAlN is superior to TiN, properties of the coating is governed by the Al content and the phase structure of the coatings. Due to this reason TiAlN coating is used in the dry and high speed machining tools with incremented tool life and reduced machine downtime [9-15]. These coatings can also be used as high-density complementary metal-oxide-semiconductor (CMOS) memory devices [16], temperature controller, solar collectors [17-20] and bio-medical implants [21]. TiAlN thin films are in general economically prepared by the magnetron sputtering method for the industrial use. Intensive study of the plasma properties of thin film is required for the growth phenomenon and various properties of the coatings. This paper is one of such studies that specifically emphasize the corresponding plasma behavior with the coating conditions.

Plasma parameter governs the feature of PVD coatings formed on the test/field substrates. To understand the exact behavior of plasma these parameter needs to be studied under continuous observations. Langmuir probe is one of the simplest probes giving most accurate result of plasma parameters. It is in use since its inception and is used for the plasma diagnostics in most of the research labs around the world. It is a tool for the direct measurement of plasma potential and current inside the deposition chambers and the current voltage (I-V) curve so obtained is used for the measurement of ion density, electron density, electron temperature and electron energy distribution function(EEDF). From the I-V curve EEDF is calculated using Druyvesteyn formula in terms of second derivative of the I-V data [1, 22-28]. Experimental and theoretic methods were employed by various authors for the measurement of plasma properties. Langmuir probe [29-32], laser induced fluorescence [33, 34] and optical emission spectroscopy (OES) [35, 36] are few of the methods used in research laboratories for plasma diagnostics.

Present work emphasizes the nature of TiAlN plasma inside the magnetron co-sputtering system and elaborates the plasma information required for the better coating conditions of field samples. Plasma energy and gas ratio based study in relation with the plasma pressure carried out in the form of I-V curve extracted by using small diameter Langmuir probe. From these studies I-V characteristics are monitored and using respective mathematical relations different parameters are calculated for plasma diagnostics [37-40].

2. Experimental setup

In the Plasma Laboratory at Birla Institute of Technology, Mesra, Ranchi RF/DC magnetron co-sputtering deposition system (Vacuum technique pvt. Ltd., Banglore) was used for the study of TiAlN plasma. It consists of dual magnetron in which pure (99.99%) Ti target is connected to DC (1kW) power supply and Al target to RF (300W) power supply, MKS type 247 mass flow controllers, sample holder and view port. Targets (50 mm diameter, 5 mm thick) were mechanically clamped to the magnetron cathode of the sputtering system. Langmuir probe of small diameter (0.5mm) and 5 mm length covered with glass sleeve inserted in the chamber from the front port as shown in the schematic diagram (Fig. 1).

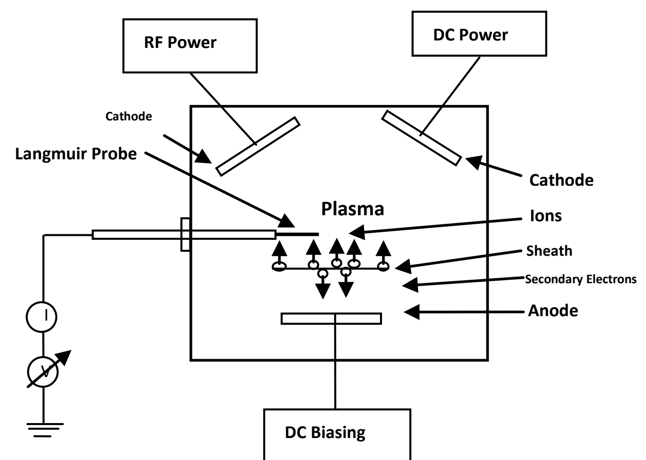

Figure 1. Schematic Diagram of RF/DC Magnetron Co-Sputtering System with Langmuir probe.

Probe is placed inside the chamber in such position that it penetrated the plasma and does not have any effect on the thin films deposited during the plasma studies. Si substrate is placed in the chamber to verify the effect of plasma parameters on the film properties. Substrates were ultrasonically cleaned for 30 minutes using

IJERT

isopropyl alcohol and dried at room temperature prior to deposition. Substrates were mounted on the sample holder and the chamber is evacuated to the base pressure of ~10^{-6} mbar. In presence of Ar target surface and the substrates were sputter etched at 100Watt power for 20min inside the deposition chamber to avoid the contamination before deposition. After sputter cleaning, Ar: N_2 gas flow rate was adjusted to 4:6 ratios and working pressure of ~ 3.5 x 10^{-2} mbar was maintained during deposition. Plasma parameters and films were obtained at different RF/DC power ratios; the deposition conditions are summarized in our earlier communication [15]. I-V characteristics curve recorded at the given power after the discharge was stabilized. Probe current measured in respect to the biasing voltage of -50 to +50Volts. Plasma parameters are calculated with the help of I-V characteristic curve and the Graphical User Interface (GUI).

3. Measurements

3.1. Plasma parameters

Langmuir probe theory is used for the study of plasma parameters. It states that when probe biasing voltage (V_B) is sufficiently negative than the plasma potential (V_P) probe collects the ion saturation current (I_{is}). Probe continuous to collect positive ion till V_B equals V_P after that probe starts repelling the ions. For $V_B \gg V_P$, current through probe is electron saturation current (I_{es}); $V_B < V_P$, probe starts partially repelling the electrons and when $V_B \ll V_P$, probe repels most of the electrons hence electron current reduces to zero (I_e =0). In case of Maxwellian electron velocity distribution, electron current decreases exponentially with decrease in biasing voltage. Using these equations we can calculate the plasma parameters [1, 26, 27, 32, 41]:

The electron current:

$$I_e(V_B) = \begin{cases} I_{es} \exp\left[-\frac{e(V_P - V_B)}{kT_e}\right], & V_B \leq V_P \\ I_{es} & , V_B > V_P \end{cases} \quad (1)$$

The electron saturation current:

$$I_{es} = en_e A\left(\frac{kT_e}{2\pi m_e}\right)^{\frac{1}{2}} \quad (2)$$

The electron temperature:

$$T_e = \frac{\partial V_B}{\partial(\ln I_e)} \quad (3)$$

Electron velocity:

$$V_e = \left(\frac{8kT_e}{\pi m_e}\right)^{\frac{1}{2}} \quad (4)$$

Ion velocity:

$$V_i = \left(\frac{8kT_e}{\pi m_i}\right)^{\frac{1}{2}} \quad (5)$$

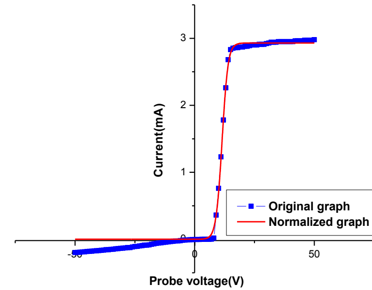

Figure 2. Langmuir probe I-V characteristics for different RF/DC power.

I-V plot was obtained after calculating true electron current by subtracting ion saturation current from total probe current. From the Langmuir I-V plot plasma potential (V_P) and floating potential (V_f) are determined (Fig. 2). Floating potential (V_f) is the potential at zero probe current and plasma potential (V_P) determined by intersection of the tangent drawn at electron saturation and electron retardation region of the In (I_e)-V plot, T_e can also be determined from the In (I_e)-V plot (Fig. 3). Energy of the bombarding particles is given by the difference of plasma potential and floating potential (V_P-V_f). Plasma potential can also be determined by zero crossing of the second derivative of I-V curve (Fig. 4).

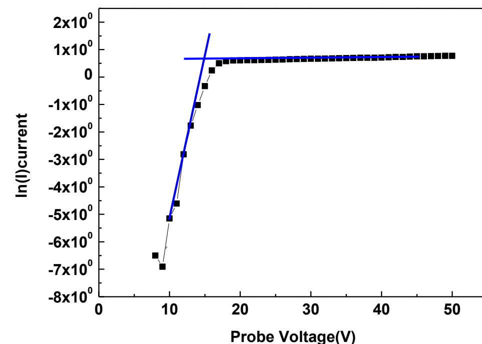

Figure 3. Variation of In (I_e) with probe voltage.

IJERT

Electron velocity is found to be nearly 10^3 times that of ion velocity. Ion velocity is in the range of 10^3 ms^{-1} while that of electron is 10^6 ms^{-1} inside the chamber. When electron temperature is considerably higher than ion temperature (Te >>Ti) the ion saturation current is determined by Bohm Sheath Criterion instead of ion thermal speed.

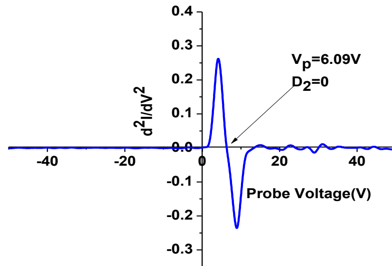

Figure 4. Variation of second derivatives of Langmuir probe trace for RF/ DC power.

The ion saturation current (I_{is}) is given as:

$$I_{is} = I_{Bohm} = 0.6eAn_i\left(\frac{kT_e}{m_i}\right)^{\frac{1}{2}} \quad (6)$$

When Te >>Ti plasma is isotropic and the probe sheath is non-collisional and thick. The area is Orbital Motion Limited (OML) region and the probe theory is OML probe theory. The ion current in the OML regime is [42]:

$$I_i = An_ie\sqrt{\left(\frac{-e(V_B - V_P)}{8m_i}\right)} \quad (7)$$

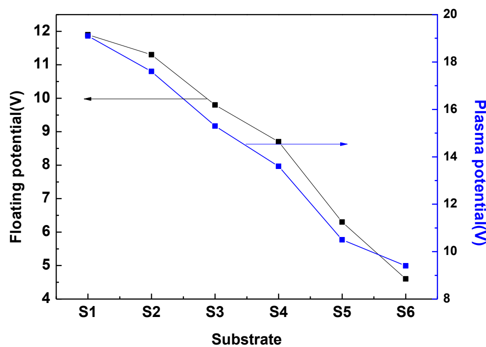

Figure 5. Variation of Plasma potential (V_p) and (V_f) with RD/DC power.

Druyvesteyn formula is used for the calculation of Electron Energy Distribution Function (EEDF), where probe current is double differentiated with respect to biasing voltage. On integration EEDF gives electron density (n_e), average electron energy ($< \varepsilon >$) and effective electron temperature ($<T_{eff}>$) [1, 26, 27, 42].

$$f_e(\varepsilon) = \frac{2m_e}{e^2A}\left(\frac{2e\varepsilon}{m_e}\right)^{\frac{1}{2}}\frac{d^2I}{dV^2} \quad (8)$$

$$n_e = \int_0^{\varepsilon \max} f_e(\varepsilon)d\varepsilon \quad (9)$$

$$< \varepsilon >= \frac{1}{n_i}\int_0^{\varepsilon \max} f_e(\varepsilon)\varepsilon d\varepsilon \quad (10)$$

$$<T_{eff}>= \frac{2}{3} < \varepsilon > \quad (11)$$

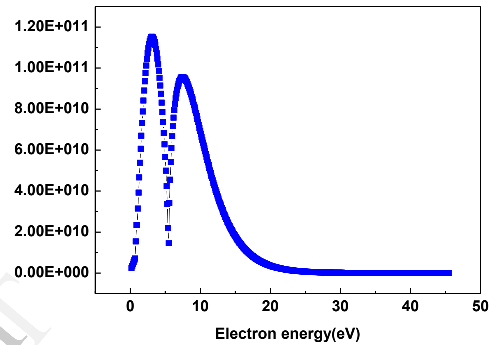

Figure 6. Normalized EEDF as a function of power ratio of 1.6(S4).

Normalized EEDFs at different RF/DC power were used to evaluate the electron density (n_e EEDF), average electron energy ⟨ ε ⟩ and effective electron temperature ⟨Teff ⟩.Fig. 6 shows the normalized EEDF as a function of energy at RF/DC power. Plasma parameters (Fig. 7), i.e., T_e, T_{eff} , V_p (slope), V_p (EEDF), V_f (slope) and particle density (Fig. 8), i.e., n_e (expt.), n_i (OML) and n_i (Bohm) are calculated from different method and at different power. The error bars in the measurements done by Langmuir probe are generally in the range of 12–17%.

3.2. Thin film characterization:

Crystallographic analyses of the deposited films were performed by GIXRD (Model: Bruker D8 Advance X-ray diffractometer). Surface morphological analysis was done by Atomic Force Microscope (AFM NT-MDT, Solver Pro 47). We have published these results in earlier communication [15]. Surface hardness of the deposited thin film is done by Nano-indenter (CETR, Bruker, DFH-5)

IJERT

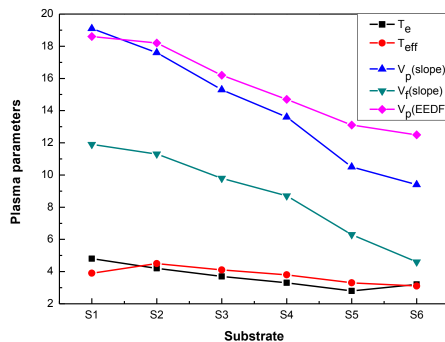

Figure7. Plasma parameters as a function of RF/DC power.

3.2.1. GIXRD analysis

The x-ray diffraction patterns obtained from the film surface (Fig. 9) shows that the film formed is polycrystalline in nature. Consisting of cubical and hexagonal TiAlN crystals in the coating matrix. It has cubic TiAlN (100) peak at (21.79) JCPDS Card no: 37-1140 and hexagonal TiAlN (114) peak placed at (68.92) JCPDS Card no: 18-0070. XRD spectra reveals that the coatings with low Al content show small hexagonal (Ti, Al) N phase and major cubic (Ti, Al) N Phase. This might have resulted due to the incorporation of cubic TiN in place of hexagonal AlN phase [15, 43].

3.2.2. Hardness Analysis

The variation of hardness and Young's modulus of the deposited films are shown in Fig. 10. It shows that the hardness varies from 10.4 GPa to 37.4 GPa and Young's modulus from 180.01 GPa to 550.82 GPa with increase in power ratio [Fig. 10]. The variation of hardness & Young's modulus of the deposited films shows that the film reached maximum hardness of 37.4 GPa. It can be inferred that when the electron temperature was higher the Ti and Al species reacted with N and the film so formed had better grain distribution as well as have maximum hardness. Atomic Force microscopy image of the sample shows even nano grains on the surface with better smoothness (Fig. 11) [15].

4. Results and discussion

The nature of the current-voltage (I-V) characteristics for different RF/DC power as shown in Fig. 2 depends not only on the plasma behavior, geometry of the Langmuir probe but also on the compensation circuit used for the RF&DC plasma investigation. System pressure is kept such that the mean free path for charge particle-neutral collision is in centimeter range whereas charged particles were collected collision free. Second derivative of the I-V curve at zero crossing was used for calculating plasma potential (Fig. 4). Constant discharge was maintained by keeping the system pressure constant by $Ar+N_2$ gas flow controlled through MFC controller. The V_p & V_f as shown in Fig. 5 gives energy of the sputtered particles bombarding the substrate. Increase in RF/DC power resulted in increased current to the cathodes, in result supplying more number of electrons in the plasma for ionization. This phenomenon is frequently observed in the magnetron sputtering system. Negative biasing of the cathode increased with increase in electron concentration in plasma causing more target material to be ejected into the plasma from the target surface. Electrons with high energy leaving the target surface follow helical motion in large gyro radius.

The electron energy distribution function f(ε), determined to check the plasma electrons Maxwellian nature using Druyvesteyn relation (Eq. 8). EEDF plot (Fig. 6) shows it is measured as a function of the probe potential V_B (taken as electron energy ε) for the plasma study. It shows that there are two peaks one at lower energy range 3.25eV and another at higher energy range 7.50eV which confirms the presence of two groups of electrons having different temperature. This type of plasma behavior is also noticed by other authors while plasma characterization and analysis. Existence of dual nature suggests that the $Ar+N_2$ plasma is non- Maxwillian. High energy electrons group arises as a result of large number of ionizing collisions between accelerated ions and neutral gas atoms producing secondary electrons due to strong electric field in vicinity of cathode. When high energy group electrons repelled by cathode returned to the plasma by virtual anode, in elastically collides with neutral gas atoms losing most of the energy and contribute as low energy electron group. The thermalization time required between the two

IJERT

groups of electrons is not enough for electrons to leave the cathode fall region and hence the electrons not able to redistribute as one Maxwellian group.

Sputter rate of a RF/DC magnetron is defined by the sputter-ejected atoms as combination of; (1) the fast moving atoms ejected from target surface and (2) movement of thermalized atoms arising due to diffusion process. By Increasing RF/DC power the number of electrons getting confined within the plasma increases; these electrons lose their energy to a greater extent during drift ionizing collisions, increasing particles density. This leads to the decrease in the electron temperature value from 4.8 to 3.2 eV (Fig. 7). Theoretically for plasma electrons to be Maxwellilan, effective electron temperature calculated from the normalized EEDF $<T_{eff}>$ should be equal the electron temperature. Here it is observed that the effective electron is slightly higher than the electron temperature [24]. The generated plasma electrons are thus non-Maxwellian having high energy tail in EEDF that strongly supports our observations.

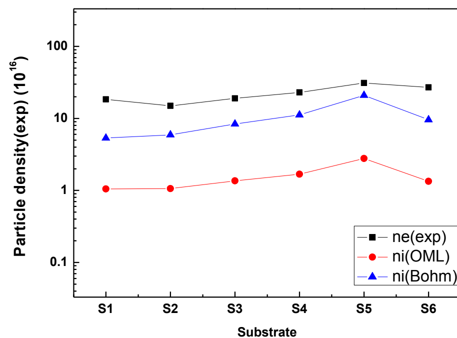

Figure 8. Particle density (n_e (expt.), n_i (OML) and n_i (Bohm)) as a function of RF/DC power.

The n_e values calculated from different methods is observed in the range 1.05×10^{16} to 1.84×10^{17} cm^{-3} with variation of applied power [Fig. 8]. In magnetron sputtering system electrons are confined to the cathode, increase in applied power results in increased sputter rate. Magnetic and electric field ($E \times B$) around the cathode present increases lifetime and the electron path. Motion of electron increases the collision probability between electron and atom causing increased ionization rate. This results in increased plasma density at increased power due to enhanced ionization with lower diffusion observed in our experimental and theoretical calculation shown in Fig. 8. Observations show fairly uniform plasma with acceptable uncertainty/errors in the measurement in the processing chamber. Other researchers have also stated in their respective works that ion-ion and ion-atom collisions within the space charge sheath surrounding the cylindrical probe influences the ion orbital motion [44].

Diffraction profile obtained from the film surface (Fig. 9) confirms the formation of TiAlN phase which is polycrystalline in nature. It is supported by the presence of the cubic TiAlN (100) peak appearing at (21.79) and hexagonal TiAlN (114) peak placed at (68.92). In the spectra it is clear that (100) phase increase with increased power and the other phase (114) reduces with the power. Spectra reveals that the small hexagonal (Ti, Al)N phase and major cubic (Ti, Al)N Phase in the coating is due to variation of Al content in the film. This phenomenon might have been resulted due to the incorporation of cubic TiN in place of hexagonal AlN phase [15, 43].

IJERT

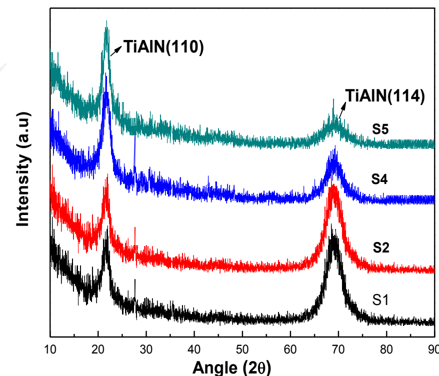

Figure 9. GIXRD diffractograms of deposited films prepared at different RF/DC power.

Nano indenter analysis shows that hardness varies from 10.4 GPa to 37.4 GPa and Young's modulus from 180.01 GPa to 550.82 GPa with increase in power ratio [Fig. 10]. Hardness & Young's modulus of the deposited films shows that the film reached maximum hardness of 37.4GPa (S4). Increase and decrease in hardness value is incorporated with the crystal nature and the Al concentration in the film. These values are maintained at predefined ratio by applying appropriate system pressure and the power/current to the cathodes. It is evident that higher concentration of (100) phase than (114) phase makes the film surface harder in comparison to lower concentration ratios. It can be inferred that

when the electron temperature was higher the Ti and Al species reacted with N and the film had better grain distribution as well as have maximum hardness.

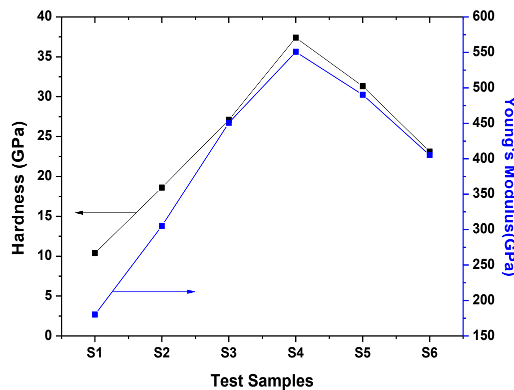

Figure 10. Variations of (a) Hardness and (b) Young's modulus of deposited films Prepared with different RF/DC power.

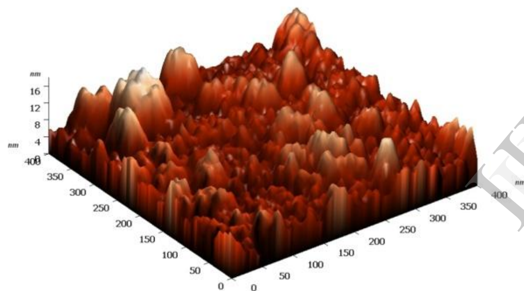

Figure 11. AFM image showing nano sized grains of Substrate (S4).

Atomic Force microscopy image of the sample shows even distribution of nano grains on the surface (Fig. 11). It is observed that the nano grains with less roughness forms smooth surface having improved surface properties.

5. Conclusion

In the present work Plasma parameter are investigated for two cathodes (RF&DC) in comparison with the TiAlN thin film properties by means of Langmuir probe. Probe parameters measurement shows existence of weak plasma region characterized by different electron density, plasma potential and temperature in relation with the applied power. It had been observed that in high plasma density region it is approximately 10^{16} - 10^{17} ions/cm^{-3}. Plasma density measured by Bohm Sheath Criterion and Orbital Motion Limited (OML) theory too confirms the same.

The deposited films crystallographic analysis shows that TiAlN nitride film with 100 and 114 orientation. Hardness analysis confirmed that when Ti, Al and N ions are in proper compositional ratio, the films have best hardness. The surface roughness and the film thickness can be improved by increasing the deposition time if more thickly and smooth films are required. In general TiAlN coating are mainly used for the hard and protective coatings and as per the nano-hardness analysis, it can be inferred that better properties are achieved at 8:5(S4) power ratio. For industrial application of reactive magnetron sputtering system, best coating can be achieved at RF/DC ratio of 1.6. Atomic Force Microscopy image confirms the surface morphology consisting of nano-grains of TiAlN that is responsible for the smoothness and hardness of the thin film.

IJERT

Acknowledgement

The authors are grateful to DST, GOI and MHRD, GOI for financial support under FIST and TEQIP respectively. The authors are also grateful to Birla Institute of Technology, Mesra, Ranchi, for providing the necessary facility and support for the present work. The authors want to acknowledge the cooperation of CIF, BIT, Mesra, Ranchi and UGC DAE consortium for Scientific Research, Indore for the characterization works. The authors want to acknowledge Dr. Mukul Gupta and Mr. Akhil Tayal, UGC DAE consortium for Scientific Research, Indore for the help in XRD study of the films reported in this paper.

References

[1] S. Z. Wu, Dependence of plasma characteristics on dc magnetron sputter parameters, Journal of applied physics 98, (2005)083301(1-5).

[2] J.A.Thronton, High rate sputtering techniques, Thin solid films 80, 1-3 (1980)1-11.

[3] J.A.Thronton and A.S.Penfold, Cylindrical magnetron sputtering thin film processes, Thin film Processes edited by J.L.Vossen and W.Kern Academic Press, New York (1978) p. 75.

[4] T.S.Kim, S.S.Park, and B.T.Lee, Characterization of nano-structured TiN thin films prepared by R.F. magnetron sputtering, Materials Letters 59(2005),3929-3932.

[5] R.Hippler, S.Pfau, M.Schmidt, K.H. Schoenbach (Eds). Low temperature Plasma Physics, Fundamental Aspects and application, Berlin; Wiley- VCH (2001).

[6] R.Hippler, H.Steffen, M.Quaas, T.Rowf, T.M.Tun, H.Wulff, In:Advances in solid state phyics, Vol 44 (Kramer B,Ed.) Springer-Verlag: Heidelberg P.299 (2004).

[7] P.Spatenka, I.Leipner, J.Vicek and J.Musil, A comparison of internal plasma parameters in a conventional planar magnetron and a magnetron with additional plasma confinement, Plasma Sources Sci-Tech. 6(1) (1997) 46-52.

[8] Roth J C, Industrial Plasma Engg. Vol 1-Principles (1995) (Bristol Institute of Physics Publishing).

[9] Munz W D, “Titanium aluminum nitride films: A new alternative to TiN coatings”. J. Vac. Sci. Technol. 4 p 2717 (1986).

[10] J.C. Oliveira, A. Manaia, A. Cavaleiro, “Hard amorphous Ti–Al–N coatings deposited by sputtering”. Thin Solid Films 516 p 5032 (2008).

[11] C. Chokwatvikul, S. Larpkiattaworn, S. Surinphong, C. Busabok, P. Termsuksawad, “Effect of Nitrogen Partial Pressure on Characteristic and Mechanical Properties of Hard Coating TiAlN Film”. Journal of Metals, Materials and Minerals 21 p 115 (2011)

[12] D.G. Park, T.H. Cha, S.H. Lee, I.S. Yeo, “Characteristics of sputtered Ti1−xAlxN films for storage node electrode barriers”. J. Vac. Sci. Technol. 19(6) p 2289 (2001).

[13] J.T. Chen, J. Wang, F. Zhang, G.A. Zhang, X.Y. Fan, Z.G. Wu, P.X. Yan, “Characterization and temperature controlling property of TiAlN coatings deposited by reactive magnetron co-sputtering”. J. Alloys compd. 472 p 91 (2009).

[14] H. C. Barshilia, N. Selvakumar, K. S. Rajam, D. V. S. Rao, K. Muraleedharan, A. Biswas, “TiAlN/TiAlON/Si3N4 tandem absorber for high temperature solar selective applications”. Appl. Phys. Lett. 89. 191909 (2006).

[15] A. K. Singh, N. Kumari, S. K. Mukherjee, P. K. Barhai, “Atomic force microscopy analysis of effect of rf/dc power ratio on the properties of co-sputtered TixAl1-xn thin films”. IJRRAS. 14(3) p 603 (2013).

[16] A. Biswas, D. Bhattacharyys, H.C. Barshilia, N. Selvakumar, K.S. Tajam, “Spectroscopic ellipsometric characterization of TiAlN/TiAlON/Si3N4 tandem absorber for solar selective applications”. Appl. Surf. Sci. 254 p 1694 (2008).

[17] H.C. Barshilia, N. Selvakumar, K.S. Rajam, A. Biswas, “Optical properties and thermal stability of TiAlN/AlON tandem absorber prepared by re active DC/RF magnetron sputtering”. Sol. Energy Mater. Sol. Cells 92 p 1425 (2008).

[18] B. Subramanian, R. Ananthakumar, M. Jayachandran, “Microstructural, mechanical and electrochemical corrosion properties of sputtered titanium-aluminum-nitride films for bio-implants”. Vacuum 85 p 601 (2010).

[19] J. Bujak, J. Walkowicz, J. Kusinski, “Influence of the nitrogen pressure on the structure and properties of (Ti,Al)N coatings deposited by cathodic vacuum arc PVD process”. Surf. Coat. Technol. 180-181 p 150 (2004).

[20] K. Chakrabarti, J.J. Jeong, S.K. Hwang, Y.C. Yoo, C.M. Lee, “Effects of nitrogen flow rates on the growth morphology of TiAlN films prepared by an rf-reactive sputtering technique”. Thin Solid Films 406 p 159 (2002).

IJERT

[21] J.H. Hsieh, C. Liang, C.H. Yu, W. Wu, "Deposition and characterization of TiAlN and multi-layered TiN/TiAlN coatings using unbalanced magnetron sputtering". Surf. Coat. Technol. 108-109 p 132 (1998).
[22] N.Y.Kim, Y.B.Son, J.H.Oh, C.K.Hwangbo and M.C.Park, TiNx layer as an antireflection and antistatic coating for display, surface and coating Technology, 128-129 (2000) 156-160.
[23] M.Nose, T.Nagae, M.Yokota, S.Saji, M.Zhou, M.Nakada, Electrical and colorimetric properties of TiN thin films prepared by DC reactive sputtering in a facing targets sputtering (FTS) system, Surface & Coating Tech. 116-119 (1999) 296-301.
[24] N.D.Cuong, D.J.Kim, B.D.Kang, C.Soo Kim and S.G.Yoon, Characterizations of high resistivity TiNxOy thin films for applications in thin film resistorsMicroelectronics Reliability 47 (2007)752-754.
[25] N.Jiang, H.J.Zhang, S.N.Bao, Y.G.Shen, Z.F.Zhou, XPS study for reactively sputtered titanium nitride thin films deposited under different substrate bias, Physica B 352 (2004) 118-126.
[26] Shu Qin & Allen MC Teer, Time-delayed, time-resolved Langmuir probe diagnostics of pulsed plasmas, Applied Phys letters 87, (2005)241506(1-3).
[27] S. B. Singh, N. Chand and D. S. Patil, Langmuir probe diagnostics of microwave electron cyclotron resonance (ECR) plasma, Vacuum 83 (2009) 372-377.
[28] F. F. Elakshar, M. A. Hassouba, and A. A. Garamoon, Measurements of the electron energy distribution Function in two different regions of dc-magnetron Sputtering device, FIZIKA A (Zagreb); 9 (2000) 177-186.
[29] S. M. Rossnagel and H. R. Kaufmann, Langmuir probe characterization of magnetron operation, J. Vac. Sci. Technol. A 4 (1986)1822-1825.
[30] T. E. Sheridan, M. J. Goeckner, and J. Goree, Observation of two-temperature electrons in a sputtering magnetron plasma, J. Vac. Sci. Technol. A 9 (1991)688-690.
[31] T. E. Sheridan, M. J. Goeckner, and J. Goree, Electron velocity distribution functions in a sputtering magnetron discharge for the E x B direction, J. Vac. Sci. Technol. A 16 (1998) 2173-2176.
[32] D. J. Field, S. K. Dew, and R. E. Burrell, Spatial survey of a magnetron plasma sputtering system using a Langmuir probe, J. Vac. Sci. Technol. A 20 (2002)2032-2041.
[33] M. J. Goeckner, J. Goree, and T. E. Sheridan, Laser-induced fluorescence characterization of ions in a magnetron plasma, J. Vac. Sci. Technol. A 8 (1990) 3920-3924.
[34] Y. W. Choi, M. Bowden, and K. Muraoka, A Study of Sheath Electric Fields in Planar Magnetron Discharges using Laser Induced Fluorescence Spectroscopy, Jpn. J. Appl. Phys., Part 1 35 (1996)5858-5861.
[35] S. Miyake, N. Shimura, T. Makabe, and A. Itoh, Diagnostics of direct-current-magnetron discharges by the emission selected computer-tomography technique, J. Vac. Sci. Technol. A 10 (1992) 1135-1139.
[36] J. E. Miranda, M. J. Goeckner, J. Goree, and T. E. Sheridan, Monte Carlo simulation of ionization in a magnetron plasma, J. Vac. Sci. Technol. A 8 (1990)1627-1631.
[37] Godyak VA, Piejak RB, Alexandrovich BM, Probe diagnostics of non-Maxwellian plasmas, J Appl Phys 73(8)(1993) 3657-3663.
[38] Druyvesteyn MJ., Hadrons and Nuclei, Z Phys A, 64 (1930)781-798.
[39] Swift JD, Schwar MJR. Electrical probes for plasma diagnostics, lliffe Books Ltd., London, (1970) Chap. 6.
[40] Cherrington BE., The use of electrostatic probes for plasma diagnostics-a review, Plasma Chem and Plasma Process, 2(2) (1982) 113-140.
[41] J. M. Hendron, C. M. O. Mahony, T. Morrow and W. G. Graham, Langmuir probe measurements of plasma parameters in the late stages of a laser ablated plume, J.Appl.Phys 81(5) (1997) 2131-2134.
[42] J. G. Watkins, D. Taussiq, R. L. Boivin, M. A. Mahdavi and R. E. Nygren, Review of Scientific Instruments, 79 (2008)10F125-128.
[43] M. Du, L. Hao, X. Liu, L. Jiang, S. Wang, F. Lv, Z. Li, J. Mi, Microstructure and thermal stability of $Ti_{1-x}Al_xN$ coatings deposited by reactive magnetron co-sputtering, Physics Procedia 18 (2011) 222-226.

IJERT

[44] N. Kumari, P. S. Das, N. K. Joshi and P. K. Barhai, Correlations of plasma parameters and properties of magnetron sputtered TiN films, Eur. Phys. J. Appl. Phys. 59 (2012) 20302-20308.

IJERT